Optics Communications 508 (2022) 127751

Contents lists available at ScienceDirect

Optics Communications

journal homepage: www.elsevier.com/locate/optcom

Fast and highly accurate estimation of feedback coupling factor and linewidth enhancement factor for displacement sensing under different feedback regimes

Muhammad Sadiq Orakzai [a], Saqib Amin [a,*], Zohaib Ahmad Khan [a], Faraz Akram [b]

[a] Department of Electrical Engineering, Faculty of Engineering & Applied Sciences, Riphah International University, Pakistan
[b] Department of Biomedical Engineering, Faculty of Engineering & Applied Sciences, Riphah International University, Pakistan

ARTICLE INFO

Keywords:
Laser feedback
Self-mixing interferometry
Feedback coupling factor
Linewidth enhancement factor
Marquardt's algorithm
Phase unwrapping
Signal processing
Laser sensor

ABSTRACT

In self-mixing interferometry, the fast and accurate estimation of fundamental feedback parameters, such as optical feedback coupling factor C and linewidth enhancement factor α, is critical for high-resolution real-time displacement sensing using an SMI sensor.

In this work, a Marquardt's algorithm (MA) based fast and highly accurate method is proposed to estimate C and α. The proposed method utilizes the SMI signal phase and applies a simple numerical analysis to estimate C and α. The proposed method can accurately estimate C and α for all three major feedback regimes (i.e., week, moderate and strong). A detailed comparison is also made with previously proposed algorithms to show the superiority of the proposed algorithm in terms of initial conditions, number of iterations, accuracy, and ability to work under all feedback regimes. The results have shown that our method has a negligible average error of around 0.0023 and 0.0006 for C and α estimation, respectively. The proposed method only requires approximately five iterations for accurate estimation. The method's simplicity, accuracy, and fast nature enable compact and cost-effective SMI sensors with high-resolution real-time displacement sensing.

1. Introduction

Self-mixing interferometry (SMI) [1,2] has been extensively applied in a range of measurement applications. Those applications includes displacement [3], velocity [4], vibration [5], angle [6], temperature [7], fluid flow rate [8], distance [9], phase [10] and refractive index [11] measurement etc. Unlike typical interferometry setup [12], SMI based sensor setup is cost-effective, compact, and self-aligned. It does not involve additional apparatuses like reference mirrors, beam splitters, or external photodetectors [1,2]. SMI signal is processed using post-processing algorithms [13] or phase unwrapping techniques [14–19] to extract desired target motion.

Usually, phase unwrapping methods (PUM's) [15–19] involve two steps processing, i.e., (1) rough phase retrieval, (2) joint estimation of fundamental optical feedback parameters of SMI laser sensor known as optical feedback coupling factor (C), and linewidth enhancement factor (α) [16]. C and α are responsible for the regime and shape of the SMI signal [16]. Accurate estimation of C and α is essential for high-resolution displacement measurement because the measurement resolution of the SMI sensor largely depends on C and α estimation [18]. Based on the C value, the SMI signal can be distributed into three major regimes, i.e., weak feedback regime (C<1), moderate feedback regime (1<=C<=4.6), and strong feedback regime (C>4.6) [20].

Therefore, many methods and techniques are used for C and α estimation leading to the measurement of target motion [13–16,21–26]. These methods can be categorized into two methods, i.e., optimization methods and SMI features (SMIF) based direct estimation methods. SMIF based methods [13,25,26] are faster than optimization-based methods, but they are only designed for specific feedback regimes and cannot process all three feedback regime signals. On the other hand, optimization-based methods [14–16,18,21–24] can process signals irrespective of their feedback regime to estimate C and α values. Some of these methods are briefly discussed below.

Zabit [21] proposed a Nelder–Mead (NM) based method to accelerate the process of C α joint estimation and provide accurate C α values for displacement retrieval. However, this method is compute-intensive and iterative. It cannot be deployed without using particular architecture or FPGA [25,27–30], compromising the cost-effectiveness and defying the real-time nature of the SMI based displacement sensing system. This method takes around 53 iterations for the joint estimation of C and α. Likewise, Fan [23] proposed a relatively more straightforward method for estimating C and α. The proposed method takes less than 11 iterations to estimate feedback parameters. Nevertheless,

* Corresponding author.
E-mail address: saqib.amin@Riphah.edu.pk (S. Amin).

https://doi.org/10.1016/j.optcom.2021.127751
Received 7 October 2021; Received in revised form 18 November 2021; Accepted 4 December 2021
Available online 8 December 2021

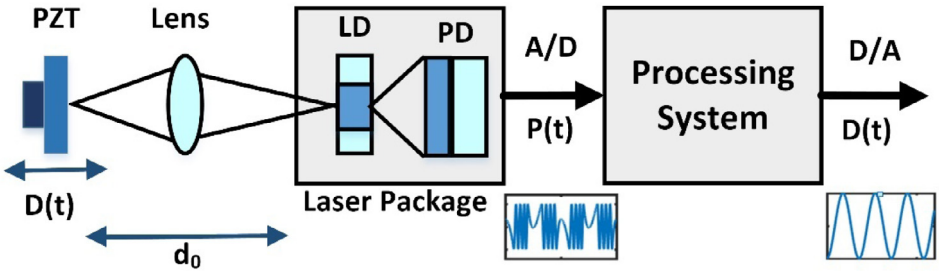

Fig. 1. Basic SMI set up for displacement retrieval.

his method was time-consuming and required many iterations to converge to optimum values, making it unsuitable for real-time low-cost displacement sensing.

Similarly, Yu et al. [31] proposed a much simpler and faster α estimation method than the previous two methods [21,23]. In the proposed method, analytical expressions for the phase segments were derived, and their graphical solution resulted in α estimation. The Results have shown an accuracy of ±6.5%. Accordingly, Ahmed et al. [22] proposed a modified Newton (MN) method-based approach to estimate C and α values quickly. The proposed Newton-based approach utilizes quadratic convergence to find an optimum solution to a nonlinear problem, which speeds up the estimation process. However, the proposed method is highly dependent on the initial guess of C and α values and may lead to high inaccuracy or even instability in some cases. Also, an increased number of iterations is required to converge if initial guesses are away from actual values, increasing computations and added time for estimating C and α parameters. This method takes less than 30 iterations to estimate C and α values.

In the context of SMIF based approach for C α estimation, Kim et al. [26] proposed a method based on features of SMI signal for C and α estimation. The proposed method utilizes the information of phase jumps, zero-crossing points, and peak points and applies algebraic operations to estimate C and α. Similarly, Chol-Man et al. [25] also proposed the SMI signal features-based method, where first-order Taylor approximation was applied to obtain mathematical relations for C and α estimation. The proposed method does not require iterations, and C α estimation can be made utilizing relations obtained from the Taylor approximation. However, both proposed methods can only work under moderate or strong feedback regimes and cannot process week feedback regime signals for C α estimation.

Similarly, Kim [13] also proposed another SMIF signal features-based method for C estimation using zero-crossing points, fringes, and max/min points of the SMI features. The proposed method has an average error of 0.02 in the estimated C value. However, this method is only designed for a week feedback regime and does not process moderate and strong feedback regime signals.

Likewise, in an optimization-based approach, Hussain et al. [24] propose a Zynq FPGA-based interferometry sensor system architecture (ISSA) for displacement retrieval using an improved phase unwrapping method (IPUM) [16]. For estimation of C and α, 10,000 iterations based brute force technique (BFT) [32] was used, where C was varied from 0 to 5 and α was varied from 0 to 10 in search of an optimum solution. FPGA provided parallel and concurrent execution of the brute force algorithm, resulting in fast and accurate estimation of C and α to at least one decimal point. However, the cost-effective nature of SMI is comprised. Similarly, Hussain et al. [18] proposed a parallel hybrid approach to implement IPUM [16] in another work. Again, a brute-force algorithm with 20,000 iterations was used for C and α estimation. The Nord-III supercomputing system was used for parallelization. The task was divided into multiple nodes, resulting in fast real-time processing of IPUM for displacement retrieval. The real-time constraints were met, but the overall cost of the system was significant due to the utilization of high computational resources.

Thus, most optimization-based methods are time-consuming and complex and require many iterations and computation power to perform C, α estimation. This increases the overall setup cost due to the utilization of particular architectures [18,24] and restricts the accuracy and real-time sensing due to the number of iterations required to estimate C and α. On the other hand, SMIF based methods do not require iterations, but they require processing extracting features from SMI signals. Furthermore, SMIF based methods can only process specific feedback regime signals for which they are designed.

So, there is a need for such a method, which can perform C and α estimation with high accuracy and minimum processing time and can process signals from all feedback regimes. Thus, this work aims to propose a fast and highly accurate C and α estimation method working under different feedback regimes.

The rest of the paper is organized as follows: the following section describes the SMI fundamentals and illustrates MA processing with the help of a block diagram. Then, Section 3 presents detailed simulated results, while Section 4 presents experimental results, followed by the conclusion.

2. SMI fundamentals and proposed methodology

This section is further divided into two subsections, namely, (1) SMI fundamentals: explaining the fundamental concept of SMI, and (2) MA Based Proposed Method: explaining MA processing for C and α estimation in detail.

2.1. SMI fundamentals

A basic understanding of SMI is required to realize the importance of C and α values in displacement retrieval using the SMI sensor and the proposed Marquardt's algorithm (MA) based method for their estimation. Fig. 1 shows an example of a typical SMI setup that utilizes a laser package composed of a laser diode (LD) and a photodiode (PD). In this setup, the target surface is a piezoelectric transducer (PZT). The focusing lens is responsible for focusing the laser beam on the target surface. The received optical output power (OOP) or SMI signal P(t) [1,2] at the sensor's output is then processed using some algorithm or PUM [15–17] for the retrieval of target displacement D(t). $P(t)$ [33] can be represented as:

$$P(t) = P_0 * [1 + m * cos(\phi_F(t))] \quad (1)$$

P_0 represents the optical output power under free-running conditions, m is the modulation index, and $\phi_F(t)$ denotes the external laser cavity feedback phase linked with target motion. Assume that is the fixed distance between the laser sensor and the stationary target surface. If the target surface is moving along the axis of the sensor with a displacement $D(t)$ and let d_0 is the fixed distance between the sensor and stationary target surface, then $\phi_F(t)$ [17] can be given as:

$$\phi_F(t) = 4\pi * \frac{d(t)}{\lambda_F(t)} \quad (2)$$

Where $\lambda_F(t)$ is the emission wavelength of the laser diode under feedback conditions, and $d(t)$ is the instantaneous distance between the target surface and the SMI sensor. $d(t)$ can be represented as [16]:

$$d\,(\mathrm{t}) = d_0 + D\,(t) = \frac{\lambda_0}{4\pi} * \phi_0(t) \tag{3}$$

Where λ_0 is emission wavelength of laser under free-running condition, and $\phi_0(t)$ is the actual or clean laser phase associated with target motion D(t) [16]. $\phi_0(t)$ can be found using the so called phase equation given by the relation [15]:

$$\phi_0\,(t) = \phi_F\,(t) + C * sin(\phi_F\,(t) + \arctan(\alpha)) \tag{4}$$

From Eq. (3), $D(t)$ is directly dependent on the accurate value of $\phi_0(t)$, and from Eq. (4), the accuracy of $\phi_0\,(t)$ is dependent on values of fundamental SMI feedback parameters C and α. Value of C factor relay on the reflectivity of the target surface and the relative distance between the SMI sensor and target surface [16]. On the other hand, the α parameter purely relies on intrinsic properties of the laser beam, such as broadening of laser beam spot and variation in frequency (chirp) [34]. Both these parameters also play an essential role in the shape of the SMI signal. The inclination of SMI fringes [20] is dependent on the α parameter, while the C parameter is responsible for the shape of the SMI signal. An increase in C value changes the shape of SMI fringes from quasi sinusoidal shape to sawtooth-like shape. The SMI signal can be categorized into three distinct feedback regimes based on the C value, namely weak feedback regime ($C \leq 1$), moderate feedback regime ($1 < C \leq 4.6$), and strong feedback regime ($C > 4.6$) [35].

Accurate estimation of both of these parameters is essential in the accurate estimation of $\phi_0(t)$, which leads to target displacement $D(t)$. Thus, any error in estimating C and α will lead to the inaccurate $D(t)$ measurement. Similarly, if the estimation of C and α is slow, then the overall process of displacement sensing will also get slower. So, there is a requirement for an accurate and fast estimation method for C and α estimation to improve the accuracy of displacement sensing and make it suitable for real-time sensing. The proposed fast and accurate estimation method is explained next.

2.2. MA based proposed method

As previously discussed, there are two types of C and α estimation techniques, i.e., optimization techniques and SMIF based techniques. The optimization methods can process different feedback regime signals but are slow due to iterative routines. On the other hand, SMIF methods are faster than previously proposed optimization methods, but they are only designed for a specific regime's SMI signals. Thus, a fast and highly accurate optimization-based method is proposed here, which can process all three major feedback regime signals.

The proposed method utilizes the Marquardt optimization algorithm (MA) [36] to estimate C and α. MA works on least square error minimization and combines gradient descent optimization and Gauss–Newton optimization methods [36]. The gradient descent method uses the steepest-descent direction to update the parameters to minimize the sum of the square of the error value of a function. So, in the case of initial guess of parameters is far from actual values. The gradient descent method will quickly converge to optimum values due to updating parameters in steepest-descent direction [36]. At the same time, convergence will be very slow when parameters approach actual values due to the limitation of the only gradient-based steepest-descent direction movement. On the other hand, the Gauss–Newton method is a quadratic optimization approach, where parameters are considered locally quadratic, and parameter updating is done by finding a minimum of quadratic. Gauss–Newton performs well when the initial guess of parameters is close to actual values while requiring more iterations when the initial guess of parameters value is far from actual values [36].

MA utilizes both the gradient descent method and Gauss–Newton method intelligently, increasing the speed of optimization and estimation accuracy. MA can estimate C and α accurately in both cases, i.e., when the initial guess is close to the actual value or is much further from the actual value. A Flowchart of MA-based proposed processing methodology is presented in Fig. 2.

MA finds the optimum solution for C and α by minimizing the sum of the least square error cost function ($J(C,\alpha)$), where $J(C,\alpha)$ is calculated using the following approach.

Let $\phi_0(n)$, $n \in N$ is a discrete version of $\phi_0(t)$, then Eq. (4) becomes:

$$\phi_0\,(n) = \phi_F\,(n) + C * sin(\phi_F\,(n) + \arctan(\alpha)) \tag{5}$$

Also,

$$\phi_0\,(n-1) = \phi_F\,(n-1) + C * sin(\phi_F\,(n-1) + \arctan(\alpha)) \tag{6}$$

Furthermore, error $E(n)$ can be calculated using the relation:

$$E\,(n) = \phi_0\,(n) - \phi_0\,(n-1) \tag{7}$$

Then the sum of the square of error or cost function $J(C,\alpha)$ will be:

$$J\,(C,\alpha) = \sum_{n=0}^{N}[E(n)]^2 = \sum_{n=0}^{N}[\phi_0\,(n) - \phi_0\,(n-1)]^2 \tag{8}$$

MA processing begins with the initial input parameters, where β is an array of coefficients to control the damping parameter (μ) value required during optimization. M is for a maximum number of iterations. At the same time, G_{tlr} is the minimum desired norm of the slope tolerance value. $X = [C_{in}, \alpha_{in}]$ is the initial guess of C and α values. Unlike the NM method [21], Newton method [22], or gradient descent method, MA performance is not affected by an initial guess. It can converge to an optimal solution even in the case of a very rough initial guess. At the beginning of each iteration, C^K and α^K values are used to process $J(C,\alpha)$ to compute the current cost function value F_1 and gradient G. Based on the norm of gradient $\|G\|$, either MA is terminated or moved to second gradient G_1 stage.

During each iteration, MA calculates a search direction (S) using Eq. (9), computes new values of C and α according to S using Eq. (10), and finds the value of the function $J(C,\alpha)$ (F_2) for these updated values.

$$S = \frac{G_1}{[G + \mu * I]} \tag{9}$$

Where G and G_1 are the first and second gradients of function $J(C,\alpha)$, respectively, while "I" is the identity matrix with dimensions equal to 2*2 (number of parameters to be estimated), using S, values of C and α in search direction will be:

$$X_S = X^K + S \tag{10}$$

Where X^K is $X = [C,\alpha]$ at kth iteration, if the square of the sum of error decreases in an iteration compared to the previous iteration, i.e., $F_2 < F_1$, this indicates a search in the right direction. As a result, μ is decreased by a factor of β [1], and $X = [C,\alpha]$ is updated with X_S, and MA behaves as Gauss–Newton method. On the other hand, $F_2 > F_1$ indicates the wrong search direction, resulting in an increase in μ by a factor of β [2], and MA behaves like a gradient descent method. MA processing concludes when desired G_{tlr} level is achieved or maximum allowable iterations are reached.

3. Simulation results

MATLAB-based simulations were performed to assess the effectiveness of the proposed algorithm. Firstly, variety of SMI signals P(t) and the associated phase $\phi_F(t)$ were generated for variable C and α values. SM simulator was used, and It was considered that, target moves with harmonic motion with a frequency $F = 3$ Hz, and peak to peak amplitude $A = 2.6\lambda_0$. Then proposed MA was evaluated for $N = 50$ K

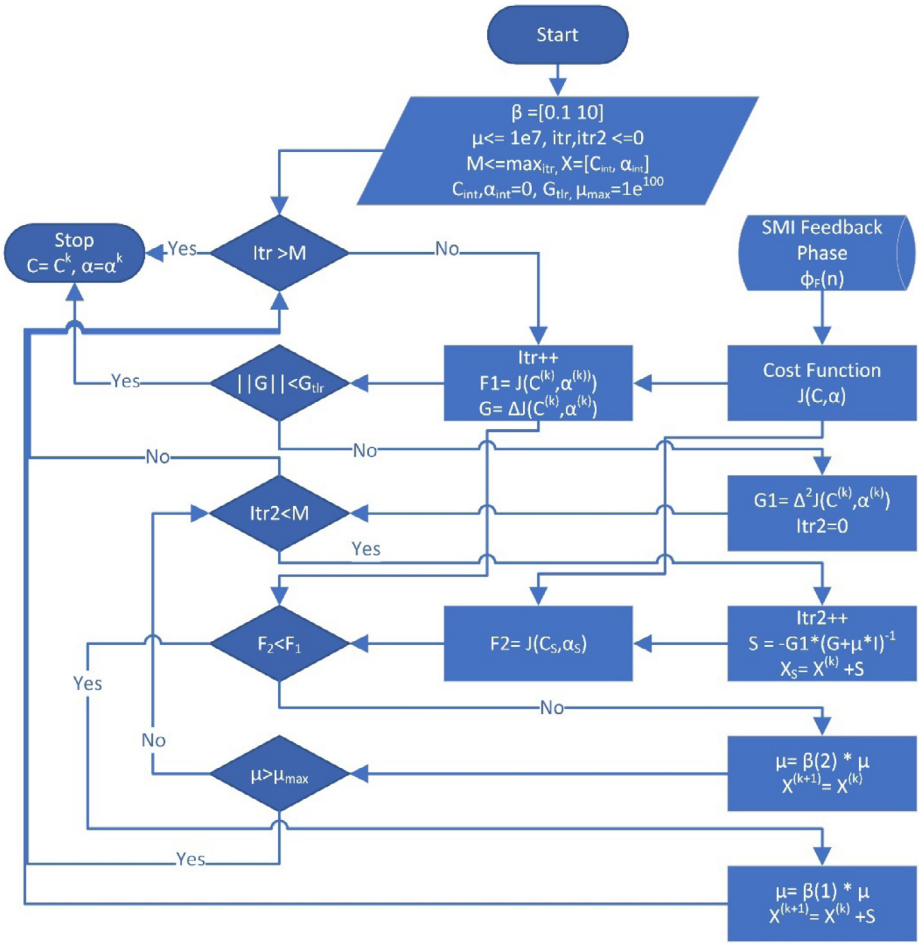

Fig. 2. Flowchart of MA-based C, α estimation method.

samples of $\phi_F(t)$ under different initial conditions of parameters using simulated signals having diverse C and α values.

The performance of the proposed MA was also compared with previously implemented and commonly used optimization methods, i.e., NM [16,21], MN [22], and Steepest descent (SD) [37] methods. $\phi_F(t)$ with $C = 0.2$ and $\alpha = 5$ was chosen for the comparison purpose. Two cases of comparison are presented in Fig. 3 and Fig. 4 respectively. Fig. 3 presents the case of choosing an initial guess near to the actual parameter values. In contrast, Fig. 4 presents the opposite case with the initial guess of parameters away from actual values.

From Fig. 3, for a signal with actual parameter values $x = [0.25]$, initial guess was chosen as $x_0 = [1–4]$. Fig. 3(1) represents the cost function (error function) values during each iteration for the proposed MA J_{MA}. The purpose of MA is to find the best combination of C, α to minimize the error function J_{MA}. The proposed MA was able to estimate actual values in only five iterations, and the final minimum possible value of J_{MA} was 4.355. (note: All the J values in Figs. 3 and 4 were calculated using Eq. (8), and then obtained results were multiplied by 1000 for a better graphical representation). MN performance was also comparable, taking seven iterations to estimate the parameters with slightly lesser accuracy. NM accuracy was also comparable with the proposed MA method. However, the NM method took 35 iterations to estimate the values. SD lagged behind all the algorithms with the poorest performance, as it took 240 iterations and accuracy was also low.

Similarly, in Fig. 4, an away initial guess of $x_0 = [6\ 6]$ was chosen for the same conditions mentioned in the previous case in Fig. 3. Again, the proposed MA estimated actual values in only six iterations with higher accuracy than other methods. NM accuracy was again comparable with the proposed MA method. However, like the last case, NM was slow in convergence and took 45 iterations to estimate the values. On the other hand, the SD method remained consistent in terms of poor accuracy and slow convergence, taking 239 iterations. The most interesting results were observed in the MN method, where NM could not converge and become unstable even after the 2nd iteration. It is due to the inherent issue with MN working well in local minimization, i.e., when the initial guess is close to the actual value, and may fail to converge when the initial guess is far away from the actual value [36]. Based on the results in Figs. 3 and 4, the proposed MA method has shown dominance over other algorithms regarding the number of iterations (speed) and accuracy.

Table 1 presents detailed simulated results for C α estimation. C was varied from 0.01 to 7, while α was varied from 0.5 to 5. Initial parameter values $x_0 = [C_0, \alpha_0]$ was chosen [1 1]. From Table 1, the average estimation error in C and α was 0.0023 and 0.0006, respectively. MA took less than six iterations on average to converge and estimate parameters with high accuracy.

The influence of noise on the proposed MA method was also observed by adding additive white Gaussian noise (AWGN) to simulated $\phi_F(t)$. Different signal-to-noise ratio (SNR) levels, i.e., 30 dB, 20 dB and 10 dB were chosen to observe the performance of MA. The approximate error in C estimation was 0.002, 0.021 and 0.086 for 30 dB, 20 dB and 10 dB respectively. Similarly, approximate error in α estimation was 0.0007, 0.032 and 0.094 for 30 dB, 20 dB and 10 dB respectively. The estimation performance of MA further degrades when SNR drops below 10 dB, such signals can be preprocessed using noise reduction methods [38–40] to improve the SNR value.

Extensive simulations were carried out for the different combinations of C and α values to compare MA with existing optimization

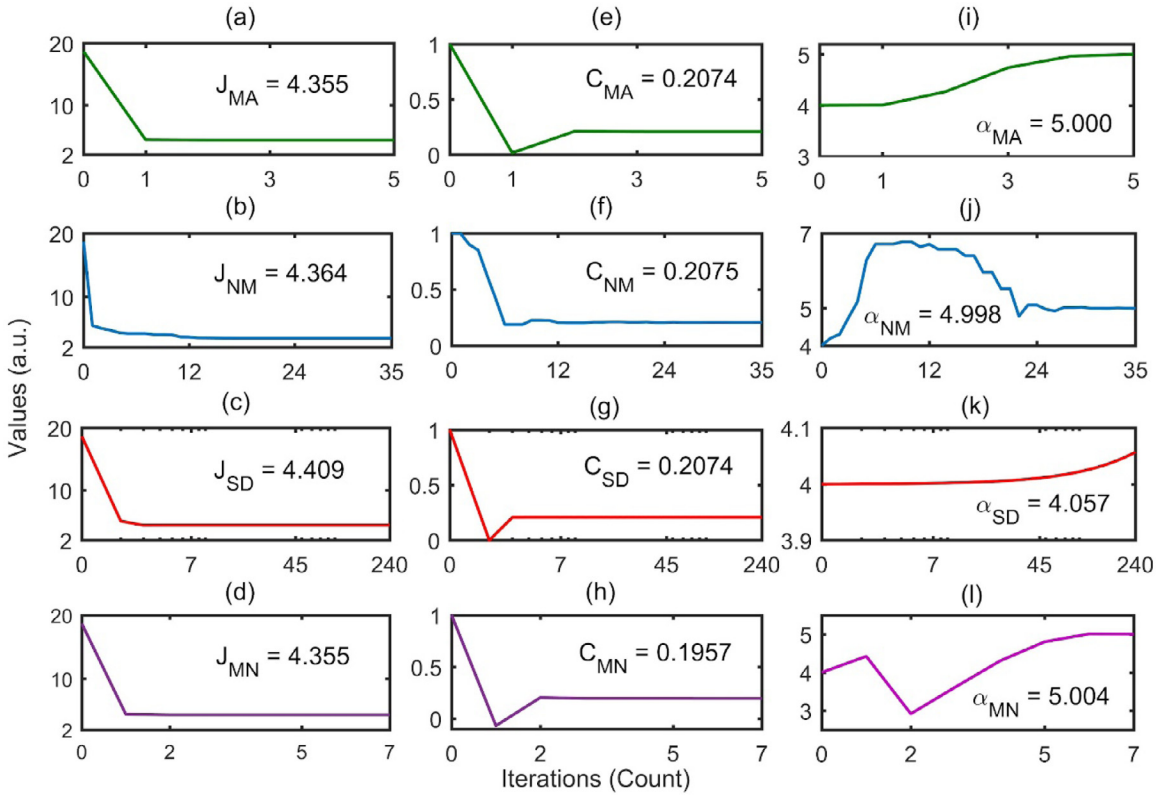

Fig. 3. Performance Comparison of estimation algorithms for initial guess near to actual parameter values. Figure shows minimization performed using (a) proposed MA (J_{MA}), (b) NM [16,21] (J_{NM}), (c) SD [37] (J_{SD}), (d) MN [22] (J_{MN}), C estimation using (e) proposed MA (C_{MA}), (f) NM (C_{NM}), (g) SD (C_{SD}), (h) MN (C_{MN}) and α estimation using (i) proposed MA (α_{MA}), (j) NM (α_{NM}), (k) SD (α_{SD}), (l) MN (α_{MN}).

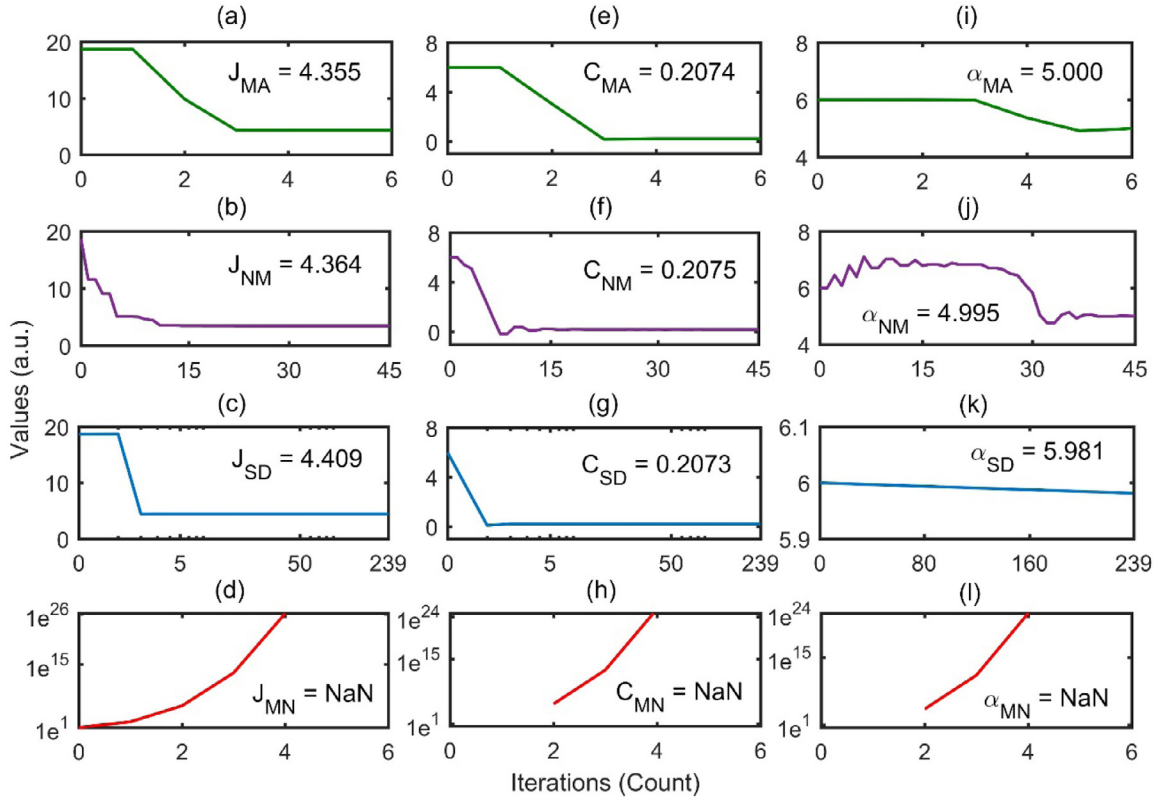

Fig. 4. Performance Comparison of estimation algorithms for initial guesses away from actual parameter values. Figure shows minimization performed using (a) proposed MA (J_{MA}), (b) NM (J_{NM}), (c) SD (J_{SD}), (d) MN (J_{MN}), C estimation using (e) proposed MA (C_{MA}), (f) NM (C_{NM}), (g) SD (C_{SD}), (h) MN (C_{MN}) and α estimation using (i) proposed MA (α_{MA}), (j) NM (α_{NM}), (k) SD (α_{SD}), (l) MN (α_{MN}).

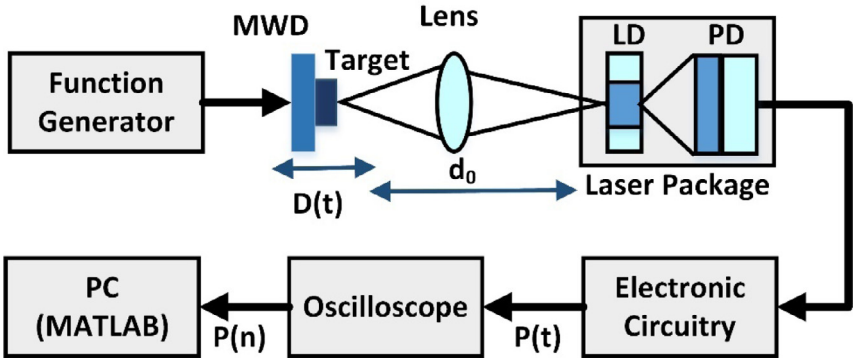

Fig. 5. Experimental Setup.

Table 1
Simulated results of C α estimation using proposed MA method for initial value x_0= [1 1].

Sr. No.	Actual values		Estimated values		Error in estimation		No. of iterations
	C	A	C_{est}	α_{est}	C_{err}	α_{err}	
1	0.01		0.016	0.499	0.006	0.001	5
2	0.4	0.5	0.407	0.500	0.007	0.000	3
3	0.8		0.804	1.000	0.004	0.000	2
4	1.6	1	1.600	1.000	0.000	0.000	5
5	2.0		2.000	1.499	0.000	0.001	5
6	2.8	1.5	2.800	1.500	0.000	0.000	5
7	3.2		3.200	2.495	0.000	0.005	5
8	4.0	2.5	4.000	2.500	0.000	0.000	3
9	4.4		4.399	3.499	0.001	0.001	7
10	5.2	3.5	5.199	3.500	0.001	0.000	5
11	5.6		5.596	4.500	0.004	0.000	6
12	6.4	4.5	6.395	4.500	0.005	0.000	6
13	7	5	6.994	5.000	0.006	0.000	8
Average estimation error					0.0023	0.0006	
Average number of iterations							5

methods and SMIF based methods [13,25,26]. The execution time of algorithms was also calculated to compare the speed of optimization methods for the IPUM [16] based Displacement retrieval. For this purpose, 50 K samples of SMI signal were processed using MATLAB on a personal computer (PC) having a 2.40 GHz i5-5th Generation processor. The speed of execution is dependent on both the processing system and the complexity of an algorithm. The originally published IPUM [16] is based on NM-based optimization and takes approximately 3.5s for displacement retrieval. SD [37] based IPUM took 4.3s for displacement retrieval, while BFT [18] based IPUM took 21.3s for displacement retrieval. Lastly, the proposed MA optimization-based IPUM took only 2.4s for displacement retrieval.

It was also observed that the optimization methods work under all three major feedback regimes with a lot of time consumption in iterative routines. MN [22] consumes approximately seven iterations and has an error of approximately 0.003 in C estimation. However, as previously discussed, MN can only minimize locally and fails to converge when the initial guess is not chosen close to actual parameter values. BFT [18] was most time-consuming as it requires 20 K iterations to estimate parameters.

Furthermore, the accuracy of BFT [18] is also low, having an approximate error of 0.099 in C estimation. More iterations are required to improve the accuracy. Similarly, NM [16,21] method took approximately 39 iterations to approximate C and α, while SD [37] took approximately 120 iterations and it failed to converge for higher values of C and α.

On the other hand, SMIF based methods only worked under specific feedback regimes, like Chol-Man [25] method only works for C>1, Kim [26] works for C>1.5, and Kim [13] works only under a weak feedback regime with C<=1, thus limits the use of SMIF based methods compared to MA-based methods. Chol-Man [25], Kim [13] and Kim [26] methods have 0.038, 0.012 and 0.08 average approximate errors in C estimation. Therefore, the accuracy of SMIF based methods is also low as compared to the proposed MA.

4. Experimental results

The proposed MA is tested using experimental SMI signals under different optical feedback regimes, linewidth enhancement factors, and target motion conditions. The schematic diagram of the SMI setup used to acquire SMI signals is shown in Fig. 5. A metal target is mounted on a PASCO SF-9324 mechanical wave driver (MWD). A GWINSTEK AFG-2225 Function generator is used to excite the target surface at different peak to peak amplitudes and frequencies ranging from 0.1 Hz – 5 KHz with the help of MWD. SMI sensor equipped with a $\lambda_0 = 658$ nm 75 mA threshold current Hitachi HL6501MG LD emitting at 35 mW of optical output power is used to acquire SMI signal. A GWINSTEK GDS2204E Oscilloscope is connected to the electronic circuitry of the SMI sensor to observe the acquired signal P(t). P(n) (digital form of P(t)) signal is transferred to a personal computer (PC) for further processing using MATLAB.

Before applying the proposed MA method, P(n) is processed using IPUM [16] based technique to obtain $\phi_F(n)$, which is then processed using MA to estimate C and α. MA was tested for a large variety of SM signal having different amplitudes and C values ranging from 0.1 to 10. Table 2 presents experimental signal based results for C estimation ($\hat{C}$) and α estimation ($\hat{\alpha}$) using proposed MA. For baseline comparison, obtained results are compared with NM method [16,21] and other optimization methods discussed in the previous section. From the results in Table 2, the accuracy of SD [37] and MN [22] is poor compared to other algorithms. While the BFT [18] based method is the slowest, consuming 20 K iterations. NM [16] accuracy is comparable with MA. However, it consumes much higher iterations than the proposed MA method.

Furthermore, the results show that the MA method can work for all three major feedback regimes, i.e., week, moderate and strong. However, in the case of a strong feedback regime (c>4.6), SMI fringes start to disappear [20], also affecting the estimation of $\phi_F(n)$ using IPUM [16]. As $\phi_F(n)$ was processed to obtain the results presented in Table 2, so error in $\phi_F(n)$ also effects C, α estimation. Simulations were carried out using simulated signals with known C value with 30 dB SNR to quantify the error performance for further increase in C value. For SMI signal with $C = 5, 6, 7, 8$ and 9 approximate error in C estimation was 0.002, 0.016, 0.058, 0.473 and 0.875 respectively.

Additionally, the performance of MA was also observed for different target amplitudes, and it was found that MA can work for SMI signals

Table 2
MA performance comparison with other methods for experimental SM signals.

Sr. No.	Amplitude (μm)	Target frequency (Hz)	MA			NM [16]			MN [22]			SD [37]			BFT [18]		
			$\hat{C}$	$\hat{\alpha}$	Itr	$\hat{C}$	$\hat{\alpha}$	Itr	$\hat{C}$	$\hat{\alpha}$	Itr	$\hat{C}$	$\hat{\alpha}$	Itr	$\hat{C}$	$\hat{\alpha}$	Itr
1	5	90	0.762	4.96	5	0.762	4.93	52	0.767	4.65	8	0.781	3.86	178	0.750	4.90	
2	1.20	40	0.912	4.98	4	0.909	4.73	57	0.914	4.66	7	0.922	4.24	135	0.900	4.90	
3	1.65	50	1.270	5.07	3	1.269	5.16	57	1.343	4.65	9	1.269	4.18	79	1.250	5.10	
4	5	160	1.350	5.03	3	1.351	5.04	57	1.363	4.66	11	1.347	4.42	79	1.350	5.10	
5	5	200	1.859	5.02	4	1.861	5.03	54	1.847	4.65	13	1.859	5.05	81	1.850	5.10	
6	5	45, 90, 225, 315	2.020	4.97	5	2.014	4.98	55	Nan	Nan	Nan	2.027	5.49	77	2.000	5.00	
7	5	90	2.069	4.99	5	2.067	5.05	55	Nan	Nan	Nan	2.072	4.52	80	2.050	5.00	20K
8	5	70, 210	2.390	5.01	5	2.387	4.94	54	Nan	Nan	Nan	2.394	4.99	81	2.400	5.00	
9	2.5	70	2.559	5.06	5	2.559	5.07	50	Nan	Nan	Nan	2.557	4.95	71	2.550	5.00	
10	5	90	3.488	5.02	5	3.486	4.97	51	Nan	Nan	Nan	3.486	5.03	62	3.500	5.10	
11	5	90	4.638	4.99	7	4.635	5.04	49	Nan	Nan	Nan	1.00	1.00	2	4.650	5.10	
12	2.5	90	6.179	4.96	9	6.178	4.94	47	Nan	Nan	Nan	1.00	1.00	2	6.200	4.90	
13	2.5	90	6.797	4.91	9	6.796	4.89	55	Nan	Nan	Nan	1.00	1.00	2	6.800	4.90	

with target motion having an amplitude above $\lambda_0/2$, because a minimum one fringe is required for estimation of $\phi_F(n)$ using IPUM [16], which is then processed using the proposed MA method.

5. Conclusion

In this work, Marquardt's algorithm-based fast and accurate C α estimation method is proposed for displacement measurement using an SMI sensor. The proposed method utilizes a simple numerical analysis approach to estimate C and α with a low average error of 0.0023 and 0.0006 for C and α estimation. The proposed method requires less than six iterations and can process SMI signals from all three major feedback regimes. The method's simplicity, accuracy, and fast nature are crucial to developing compact and cost-effective SMI sensors with high-resolution real-time displacement sensing.

Declaration of competing interest

The authors declare that they have no known competing financial interests or personal relationships that could have appeared to influence the work reported in this paper.

References

[1] S. Donati, Developing self-mixing interferometry for instrumentation and measurements, Laser Photonics Rev. 6 (3) (2012) 393–417.
[2] T. Taimre, M. Nikolić, K. Bertling, Y.L. Lim, T. Bosch, A.D. Rakić, Laser feedback interferometry: a tutorial on the self-mixing effect for coherent sensing, Adv. Opt. Photonics 7 (3) (2015) 570–631.
[3] O.D. Bernal, H.C. Seat, U. Zabit, F. Surre, T. Bosch, Robust detection of non-regular interferometric fringes from a self-mixing displacement sensor using Bi-wavelet transform, IEEE Sens. J. 16 (22) (2016) 7903–7910.
[4] X. Wang, B. Gao, C. Jiang, T. Dong, P. Chen, All-fiber rotary velocity measurement based on Doppler frequencies difference obtained by two homodyne interferometers, Appl. Opt. (2021).
[5] M. Norgia, F. Bandi, A. Pesatori, S. Donati, High-sensitivity vibrometer based on FM self-mixing interferometry, J. Phys. Conf. Ser. 1249 (1) (2019) 012020.
[6] Y. Zhao, H. Zhang, Angle measurement method based on speckle affected laser self-mixing interference signal, Opt. Commun. 482 (2021) 126569.
[7] Y. Zhao, J. Zhou, C. Wang, Y. Chen, L. Lu, Temperature measurement of the laser cavity based on multi-longitudinal mode laser self-mixing effect, IEEE Sens. J. 19 (12) (2019) 4386–4392.
[8] C. Bourquard, A. Faure-Beaulieu, N. Noiray, Whistling of deep cavities subject to turbulent grazing flow: intermittently unstable aeroacoustic feedback, J. Fluid Mech. 909 (2021).
[9] Z. Duan, Y. Yu, B. Gao, C. Jiang, Absolute distance measurement based on multiple self-mixing interferometry, Opt. Commun. 389 (2017) 270–274.
[10] C. Wang, et al., Full-circle range and microradian resolution angle measurement using the orthogonal mirror self-mixing interferometry, Opt. Express 26 (8) (2018) 10371–10381.
[11] Y. Zhang, Y. Wei, C. Chen, W. Huang, X. Wang, H. Xu, Self-mixing interferometer based on frequency analysis method for accurate refractive index measurement, IEEE Photonics J. 8 (2) (2016) 1–6.
[12] J.V. Knuuttila, P.T. Tikka, M.M. Salomaa, Scanning michelson interferometer for imaging surface acoustic wave fields, Opt. Lett. 25 (9) (2000) 613–615.
[13] C.-H. Kim, Effect of linewidth enhancement factor on displacement reconstruction and immediate estimation of feedback factor for weak feedback, Opt. Commun. 461 (2020) 125203.
[14] A.L. Arriaga, F. Bony, T. Bosch, Real-time algorithm for versatile displacement sensors based on self-mixing interferometry, IEEE Sens. J. 16 (1) (2016) 195–202.
[15] C. Bes, G. Plantier, T. Bosch, Displacement measurements using a self-mixing laser diode under moderate feedback, IEEE Trans. Instrum. Meas. 55 (4) (2006) 1101–1105.
[16] O.D. Bernal, U. Zabit, T. Bosch, Study of laser feedback phase under self-mixing leading to improved phase unwrapping for vibration sensing, IEEE Sens. J. 13 (12) (2013) 4962–4971.
[17] U. Zabit, O.D. Bernal, S. Amin, M.F. Qureshi, A.H. Khawaja, T. Bosch, Spectral processing of self-mixing interferometric signal phase for improved vibration sensing under weak-and moderate-feedback regime, IEEE Sens. J. 19 (23) (2019) 11151–11158.
[18] T. Hussain, S. Amin, U. Zabit, E. Ayguadé, Implementation of a high-accuracy phase unwrapping algorithm using parallel-hybrid programming approach for displacement sensing using self-mixing interferometry, J. Supercomput. 77 (9) (2021) 9433–9453, http://dx.doi.org/10.1007/s11227-021-03634-6.
[19] S. Amin, T. Hussain, Improved displacement sensing by spectral processing of laser self-mixing interferometry signal phase, Optik (2021) 167722.
[20] S. Amin, U. Zabit, O.D. Bernal, T. Hussain, High resolution laser self-mixing displacement sensor under large variation in optical feedback and speckle, IEEE Sens. J. (2020).
[21] U. Zabit, Optimisation of a Self-Mixing Laser Displacement Sensor, 2010.
[22] I. Ahmed, U. Zabit, Fast estimation of feedback parameters for a self-mixing interferometric displacement sensor, in: 2017 International Conference on Communication, Computing and Digital Systems, C-CODE, IEEE, 2017, pp. 407–411.
[23] Y. Fan, Improvement of measurement performance for self-mixing interferometry based displacement sensing system, 2011.
[24] T. Hussain, S. Amin, U. Zabit, O.D. Bernal, T. Bosch, A high performance real-time interferometry sensor system architecture, Microprocess. Microsyst. 64 (2019) 23–33.
[25] C.-M. Ri, C.-H. Kim, Y.-N. Oh, S.-C. Kim, Immediate estimation of feedback factor and linewidth enhancement factor from measured self-mixing signals under moderate or strong regime, Meas. Sci. Technol. 31 (6) (2020) 065204.
[26] C. Kim, C. Lee, O. Kwonhyok, Effect of linewidth enhancement factor on fringe in a self-mixing signal and improved estimation of feedback factor in laser diode, IEEE Access 7 (2019) 28886–28893.
[27] S. Amin, T. Hussain, U. Zabit, FPGA based processing of speckle affected self-mixing interferometric signals, in: 2016 International Conference on Frontiers of Information Technology, FIT, IEEE, 2016, pp. 292–296.
[28] S. Amin, U. Zabit, T. Hussain, O.D. Bernal, Hardware implementation of metric algorithms for a self-mixing laser interferometric sensor, in: 2016 19th International Multi-Topic Conference, INMIC, IEEE, 2016, pp. 1–5.
[29] T. Hussain, S. Amin, U. Zabit, F. Kamran, O.D. Bernal, T. Bosch, A high performance real-time FGPA-based interferometry sensor architecture, in: 2016 International Conference on Frontiers of Information Technology, FIT, IEEE, 2016, pp. 130–135.
[30] T. Hussain, S. Amin, U. Zabit, Implementation of high precision laser interferometry algorithm for real-time displacement sensing using multi-core architecture, in: 2017 International Conference on Communication, Computing and Digital Systems, C-CODE, IEEE, 2017, pp. 369–373.
[31] Y. Yu, G. Giuliani, S. Donati, Measurement of the linewidth enhancement factor of semiconductor lasers based on the optical feedback self-mixing effect, IEEE Photonics Technol. Lett. 16 (4) (2004) 990–992.
[32] D.J. Bernstein, Understanding Brute Force, Vol. 36, Workshop Record of ECRYPT STVL Workshop on Symmetric Key Encryption, eSTREAM report, Citeseer, 2005, p. 2005.

[33] Y. Zhao, X. Fan, C. Wang, L. Lu, An improved intersection feedback micro-radian angle-measurement system based on the laser self-mixing interferometry, Opt. Lasers Eng. 126 (2020) 105866.
[34] K. Kou, C. Wang, Influence of linewidth enhancement factor $$\alpha $$ α on self-mixing interferometry in solid-state lasers, Opt. Rev. 28 (1) (2021) 99–105.
[35] H.-S. Hong, C.-H. Kim, J.-H. Kim, U.-H. Song, H.-S. Li, K.-I. Mun, High-speed joint estimation of for strong feedback regime with fringe loss, Opt. Commun. 474 (2020) 126161.
[36] H.P. Gavin, The Levenberg–Marquardt Algorithm for Nonlinear Least Squares Curve-Fitting Problems, Department of Civil and Environmental Engineering, Duke University, 2019, p. 1.
[37] J.C. Meza, Steepest descent, Wiley Interdiscip. Rev. Comput. Stat. 2 (6) (2010) 719–722.
[38] I. Ahmed, U. Zabit, A. Salman, Self-mixing interferometric signal enhancement using generative adversarial network for laser metric sensing applications, IEEE Access 7 (2019) 174641–174650.
[39] Z.A. Khan, U. Zabit, O.D. Bernal, T. Hussain, Adaptive estimation and reduction of noises affecting a self-mixing interferometric laser sensor, IEEE Sens. J. 20 (17) (2020) 9806–9815.
[40] S. Donati, M. Norgia, SNR improvement of 8.2 dB in a self-mixing laser diode interferometer by using the difference signal at the output mirrors, Chin. Opt. Lett. 19 (9) (2021) 092502.